Effects of intramolecular dipolar coupling on the isotropic-nematic phase transition of a hard spherocylinder fluid

David C. Williamson,* Neil A. Thacker, and Stephen R. Williams
Imaging Science and Biomedical Engineering, Stopford Building, University of Manchester, Oxford Road, Manchester M13 9PT, United Kingdom
(Received 28 April 2004; revised manuscript received 23 August 2004; published 8 February 2005)

The thermodynamics of a simple model, containing the minimum set of features required to provide liquid crystal-like phase behavior and the dipolar coupling observable in the NMR spectrum of orientationally ordered fluids, are presented within the framework of Onsager theory. The model comprises a fluid of hard spherocylinders with a pair of embedded freely rotating magnetic dipoles. The behavior of the isotropic-nematic phase transition is explored as a function magnetic field strength and of the relative orientation between the nematic director and the external magnetic field. When the field and director are aligned the phase diagram is similar to those predicted for a hard rod fluid in flow fields, electric fields, and magnetic fields, with the field promoting orientational order in the fluid and the isotropic-nematic phase transition being replaced by a paranematic-nematic phase transition. In contrast, when the field and director are perpendicular, the field destabilizes the nematic phase and the phase transition is shifted to higher densities. The variation of the mean magnetic moment and the dipolar coupling are examined as a function of the orientational structure of the fluid. The model is used to support the hypothesis that dipolar couplings observed in the spectra of human leg muscle originate from nematiclike liquid crystal phases in relatively small metabolite molecules. The fitted theoretical predictions of the dependence of the dipolar coupling on the orientation of the field with respect to the nematic director are shown to provide a good description of the experimental data.

DOI: 10.1103/PhysRevE.71.021702 PACS number(s): 64.70.Md, 05.20.−y

INTRODUCTION

NMR spectroscopy is used to determine molecular composition and conformation. Of particular interest for the determination of molecular structure is the intramolecular dipolar coupling between magnetic dipoles. In an isotropic fluid this coupling averages to zero through random free rotation. However, in an ordered fluid, such as a nematic liquid crystal, the dipole-dipole coupling becomes nonzero and results in peak splitting in the NMR spectrum [1]. Experiments are usually carried out in which a sample of the molecule of interest is dissolved in a liquid crystal solvent. The aligned solvent restricts the rotational motion of the molecules, imparting weak orientational order to the solute molecules. This weak orientation is used to determine the alignment of the particular chemical bonds connecting two moieties that are visible to NMR.

In contrast to its application in analytical chemistry, in an *in vivo* NMR spectroscopy experiment the molecules of interest are usually well known, however, the biological environment in which the molecules are contained is less well understood. As such, one of the challenges of MR spectroscopy should be to probe the biological environment, a hypothesis recently discussed by Boesch [2]. In particular, the dipolar coupling resulting from orientational ordering has been observed for metabolites in skeletal muscle [3–7].

Recently Sandström and co-workers demonstrated how statistical mechanics, in the form of molecular dynamics simulations [8,9], could be used to interpret NMR spectra in terms of detailed structural information about a molecule. However, the complexity of the biological environment makes the use of atomistic molecular dynamics much less feasible. As a result, the object of this work is to provide a simplified model into which more detailed interactions can be built. The two most important features in the model are the inclusion of the intramolecular dipolar coupling and a fluid that will form an ordered mesophase. The simplest manner of promoting orientational order into a fluid is through anisotropy in the harsh, short-ranged repulsive interactions. In 1949 Onsager provided a theory for a fluid of hard rods [10]. The theory predicted that at a sufficiently high density the hard rod fluid would spontaneously undergo a phase transition from the isotropic phase to the orientational ordered nematic phase. Here, we examine a fluid of hard spherocylinders, a cylinder of length L and diameter D capped by a hemispherical cap also of diameter D. The spherocylinder fluid is used because the thermodynamics of this fluid have been studied in detail and its phase diagram carefully mapped [11,12].

Two freely rotating magnetic dipoles are embedded in the spherocylinders. Dipoles in the same molecule interact through the direct dipolar coupling. However, dipoles in different molecules do not interact. The fluid is exposed to an external magnetic field that interacts with the dipoles. The thermodynamic and magnetic properties of the fluid are obtained using Onsager's theory in both the isotropic and nematic phases.

THEORY

Consider an ensemble of N spherocylinders that are confined to a volume V at a constant temperature T. The sphero-

*Present address: Department of Chemistry, University of Manchester, Oxford Road, Manchester, M13 9PT, United Kingdom. Email address: david.c.williamson@manchester.ac.uk

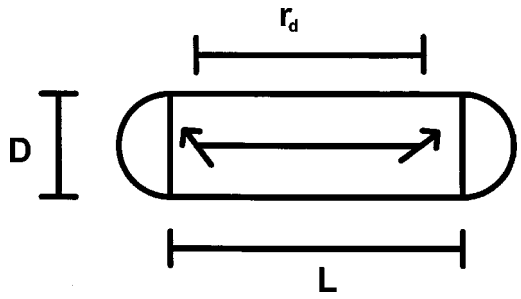

FIG. 1. Schematic representation of the spherocylinder model. The spherocylinder comprises a cylinder of length L and diameter D capped by two hemispherical caps of diameter D. Embedded in the spherocylinder are two magnetic dipoles, represented by the two arrows. The dipoles are free to rotate and their centers lie on the center line of the cylinder. They are separated by a distance r_d.

cylinders interact with each other through the following pairwise potential:

$$U(\overline{r_{i,j}},\hat{\Omega}_i,\hat{\Omega}_j)=\begin{cases}\infty, & \overline{r_{i,j}}\in V_{ex}(\hat{\Omega}_i,\hat{\Omega}_j)\\ 0 & \text{otherwise.}\end{cases} \tag{1}$$

Here $\overline{r_{i,j}}$ is the vector joining the centers of mass of two spherocylinders i and j and $\hat{\Omega}_j$ is the unit vector describing the orientation of molecule j. $V_{ex}(\hat{\Omega}_i,\hat{\Omega}_j)$ is the excluded volume between two molecules with fixed orientation.

Embedded in each spherocylinder are two permanent magnetic dipoles. The centers of the dipoles lie on the center line of the spherocylinder and are separated by the distance r_d, see Fig. 1. The dipoles are free to rotate and couple to an external magnetic field $\mathbf{B}_o$ as

$$U^D(\theta_B)=-\mu B_0\cos\theta_B. \tag{2}$$

Here, μ is the magnitude of the dipole moment, B_o is the magnitude of the external field, and θ_B is the angle between the dipole vector and the field.

In addition to this coupling, each pair of dipoles in a molecule are coupled through the usual direct dipole-dipole coupling,

$$U^{DD}(\hat{\Omega}_i,\hat{\Omega}_1,\hat{\Omega}_2)=-\frac{\mu_0\mu^2}{4\pi r_d^3}[3(\hat{\Omega}_i\cdot\hat{\Omega}_1)(\hat{\Omega}_i\cdot\hat{\Omega}_2)-(\hat{\Omega}_1\cdot\hat{\Omega}_2)]. \tag{3}$$

Here Ω_i is the vector joining the centers of the dipoles and μ_0 is permeability. In this case the dipole-dipole vector has the same orientation as the molecule in which the dipoles are embedded. Ω_1, and Ω_2 are the orientations of the two dipoles. In common with other theoretical work involving magnetic dipoles, it is assumed that dipoles in different molecules do not interact [13,14]. As a direct result of this assumption, the magnetic dipoles are influenced by the orientational structure of the hard spherocylinder fluid but are independent of the position of the molecular centers of mass. As a consequence the theory, in regard to the dipolar interactions, does not differentiate between the nematic phase and an orientationally ordered phase with additional positional order such as the smectic phases.

In this work we use the idea of treating molecules of a particular orientation as a distinct species [10] in conjunction the assumption that magnetic dipoles in different molecules do not interact to derive an expression for the Helmholtz free energy of the dipolar spherocylinder fluid,

$$\begin{aligned}\frac{A}{NkT}=&\int f(\hat{\Omega}_i)\ln f(\hat{\Omega}_i)d\hat{\Omega}_i+\int\rho(\hat{\Omega}_1)\ln\rho(\hat{\Omega}_1)d\hat{\Omega}_1+\frac{A^{ideal}}{NkT}\\&+\int\int\int\frac{A_1^{DD}(\hat{\Omega}_i,\hat{\Omega}_1,\hat{\Omega}_2)}{kT}\\&\times\rho(\hat{\Omega}_1)\rho(\hat{\Omega}_2)f(\hat{\Omega}_i)d\hat{\Omega}_1d\hat{\Omega}_2d\hat{\Omega}_i\\&+\int\int\frac{A^{excess}(\hat{\Omega}_i,\hat{\Omega}_j)}{NkT}f(\hat{\Omega}_i)f(\hat{\Omega}_j)d\hat{\Omega}_id\hat{\Omega}_j.\end{aligned} \tag{4}$$

The details of the derivation are given in Appendix A. The first and last terms correspond to the free energy due to the spherocylinders, while the second and fourth correspond to the dipole contribution and the third term is the ideal gas contribution.

The ideal gas contribution is given by

$$\frac{A^{ideal}}{NkT}=\left[\ln\left(\frac{N}{V}\right)-1+\ln\left(\frac{h^2}{2\pi mkT}\right)^{3/2}\right], \tag{5}$$

where h is the Planck constant and m is the mass of a particle. The derivation of this term can be found in any standard statistical mechanics text book, e.g., Ref. [15].

The free energy contribution due to the hard spherocylinders, as derived by Onsager [10], is

$$\begin{aligned}&\int f(\hat{\Omega}_i)\ln[f(\hat{\Omega}_i)]d\Omega_i\\&+\int\int\frac{A^{excess}(\hat{\Omega}_i,\hat{\Omega}_j)}{NkT}f(\hat{\Omega}_i)f(\hat{\Omega}_j)d\hat{\Omega}_id\hat{\Omega}_j=\sigma[f]+C\rho[f]\end{aligned} \tag{6}$$

with

$$\sigma[f]=\int f(\hat{\Omega}_i)\ln f(\hat{\Omega}_i)d\hat{\Omega}_i \tag{7}$$

and

$$\rho[f]=\frac{4}{\pi}\int\int\sin\gamma(\hat{\Omega}_i,\hat{\Omega}_j)f(\hat{\Omega}_i)f(\hat{\Omega}_j)d\hat{\Omega}_id\hat{\Omega}_j, \tag{8}$$

where $\gamma(\hat{\Omega}_i,\hat{\Omega}_j)$ is the angle between the molecular orientation of spherocylinder i and j and $C=(L/D)\eta$ where η is the packing fraction $N\nu_o/V$ and v_o is the cylinder volume $\pi D^2L/4$.

It is worth noting that the Onsager free energy is an accurate description of the thermodynamics of a fluid of hard spherocylinders only when the spherocylinder length is sufficiently large to drive the isotropic-nematic phase transition to low densities, where the higher order terms in the virial expansion become negligible. For shorter rods the Onsager formalism is less accurate. However, it is known that the

Onsager free energy does reproduce the salient features of the phase diagram, with the added advantage that the spherocylinder length and the packing fraction are coupled in a single parameter. It is possible to obtain a more accurate expression for the Helmholtz free energy using the decoupling approximation of Parsons [25], however, this approach does not affect the general features of the phase diagram. Since the aim of this work is to investigate the effects of the intramolecular dipole-dipole coupling on the isotropic-nematic phase transition and the effects of nematic ordering on the NMR spectrum of a model fluid the Onsager formalism should provide a suitable framework.

The final contribution to the free energy comes from the intramolecular interaction between the dipoles embedded in a molecule and the coupling of the dipoles to an external magnetic field. We will deal with this contribution in more detail.

At fixed dipole and molecular orientation, the energy of one molecule in the magnetic field $\mathbf{B}_o$ is given by

$$U(\hat{\Omega}_i,\hat{\Omega}_1,\hat{\Omega}_2) = -B_o\mu\cos\theta_{B1} - B_o\mu\cos\theta_{B2} - \frac{\mu_0\mu^2}{4\pi r_d^3}[3(\hat{\Omega}_i\cdot\hat{\Omega}_1)(\hat{\Omega}_i\cdot\hat{\Omega}_2) - (\hat{\Omega}_1\cdot\hat{\Omega}_2)], \tag{9}$$

where θ_{Bk} is the angle between the magnetic field and the dipole k. The single particle partition function can then be obtained through

$$Q_1^{DD}(\hat{\Omega}_i,\hat{\Omega}_1,\hat{\Omega}_2) = \exp\left(-\frac{U(\hat{\Omega}_i,\hat{\Omega}_1,\hat{\Omega}_2)}{kT}\right). \tag{10}$$

The Helmholtz free energy can now be obtained by using the usual thermodynamic relationship

$$\frac{A_1^{DD}(\hat{\Omega}_i,\hat{\Omega}_1,\hat{\Omega}_2)}{kT} = -\frac{B_o\mu}{kT}\cos\theta_{B1} - \frac{B_o\mu}{kT}\cos\theta_{B2} - \frac{\mu_0\mu^2}{4\pi r_d^3 kT}[3(\hat{\Omega}_i\cdot\hat{\Omega}_1)(\hat{\Omega}_i\cdot\hat{\Omega}_2) - (\hat{\Omega}_1\cdot\hat{\Omega}_2)]. \tag{11}$$

The free energy of the full fluid is obtained from the weighted integral of Eq. (16)

$$\frac{A_1^{DD}}{kT} = -\frac{B_o\mu}{kT}\int\cos\theta_{B1}\rho(\hat{\Omega}_1)d\hat{\Omega}_1 - \frac{B_o\mu}{kT}\int\cos\theta_{B2}\rho(\hat{\Omega}_1)d\hat{\Omega}_1 - \frac{\mu_0\mu^2}{4\pi r_d^3 kT}\int\int\int[3(\hat{\Omega}_i\cdot\hat{\Omega}_1)(\hat{\Omega}_i\cdot\hat{\Omega}_2) - (\hat{\Omega}_1\cdot\hat{\Omega}_2)] \times\rho(\hat{\Omega}_1)d\hat{\Omega}_1\rho(\hat{\Omega}_1)d\hat{\Omega}_1 f(\hat{\Omega}_i)d\hat{\Omega}_i. \tag{12}$$

It is clear from Eq. (4) that the Helmholtz free energy is a functional of the dipole orientational distribution function (DODF) and the molecular orientational distribution function (MODF). At this point we introduce the following function for the DODF:

$$\rho(\hat{\Omega}_1) = \frac{\alpha}{\sinh(\alpha)}\exp[\alpha\cos(\theta_{B1})], \tag{13}$$

where θ_{B1} is the angle between the direction of the external field and the dipole orientation and α is a variable parameter. This form of the DODF has been chosen because it is the exact solution for the free energy minimization of free noninteracting dipole, this derivation is provided in Appendix B. Substituting this function into Eq. (12) and setting the dipolar coupling to zero, as is the case in the isotropic phase, gives the exact Langevin free energy [13–15] with

$$\alpha = \frac{nB_o\mu}{kT}, \tag{14}$$

where n is the number of dipoles per molecule. In the nematic phase the dipolar coupling term in Eq. (12) is nonzero and since it depends on DODF, it is clear that Eqs. (13) and (14) are not necessarily the analytical solution to the minimization of the free energy with respect to $\rho(\hat{\Omega}_1)$. However, since the dipole moment appears in the dipolar coupling term as a square, this term cannot promote antiparallel alignment of the dipoles. As such the dipolar term either promotes dipolar ordering if the contribution to the free energy is negative, or promotes dipolar disorder if the free energy contribution is positive. The sign of the dipolar coupling term is determined by the angle between the field and the nematic director. The limits of dipolar ordering remain the same as the isotropic case, namely total disorder or full alignment. The DODF describes the probability of finding a dipole at a given orientation and the functional form in Eq. (13) has already been shown to describe the limiting distributions. As mentioned above, the dipolar coupling term does not promote any new orientational behavior of the dipole system, rather it perturbs the existing orientation order, and as such it seems reasonable that the shape of the distribution function will be similar to that found in the isotropic phase. However, the effects of the dipolar coupling are such that at a given set of parameters, N, V, T, μ, B_0, r_d, the value of α that minimises the free energy will not be the value given in Eq. (14). With the intramolecular dipolar coupling included it becomes necessary to determine α by minimizing the free energy for each set of parameters, N, V, T, μ, B_0, r_d. Substituting Eq. (13) into Eq. (12), expanding the dot products and integrating over the dipole orientations gives

$$\frac{A_1^{DD}}{kT} = \frac{2\mu B_0}{kT}L(\alpha) - \frac{\mu_0\mu^2}{4\pi r_d^3 kT}L(\alpha)^2 \times\int P_2(\cos\theta_B(\hat{\Omega}_i))f(\hat{\Omega}_i)d\hat{\Omega}_i. \tag{15}$$

Here $\theta_B(\Omega_i)$ is the angle between the external field and the molecular orientation, $L(\alpha)$ is the Langevin function, $(\coth\alpha - 1/\alpha)$ and $P_2(x)$ is the second Legendre polynomial. The two orientations are coupled because the integration over the dipole orientations has been carried out under the assumption that the external field coincides with the z direc-

tion of an arbitrary Cartesian coordinate framework. Equation (13) must also be substituted into the second term in Eq. (4) and the necessary integrals performed, giving

$$\int \rho(\hat{\Omega}_1)\ln \rho(\hat{\Omega}_1)d\hat{\Omega} = \ln\left(\frac{\alpha}{\sinh \alpha}\right) + \alpha L(\alpha). \quad (16)$$

The minimization of the Helmholtz free energy with respect to the DODF determines the magnetic properties of the fluid. In addition the orientational structure of the fluid must be determined by minimizing the free energy with respect to the MODF. To do this we follow the method proposed by Lasher [16] and described in detail by Lekkerkerker *et al.* [17] in their review of Onsager theory [18]. The nematic phase, by definition, is cylindrical symmetric, therefore the MODF only depends on the polar angle of the molecules. It is possible to describe the MODF with a particular functional form and a single variable parameter as proposed by Onsager. However, the assumption of a particular functional form has been shown to overestimate the orientational order and transition densities at the isotropic-nematic phase transition [17]. On the other hand, as suggested by Lasher [16], the MODF can be represented as a Legendre series with unknown coefficients,

$$f(\theta_i) = \sum_{n=0}^{\infty} a_{2n}P_{2n}(\cos\ \theta_i). \quad (17)$$

This expansion is appropriate for any functional form with the symmetry properties described above, thus removing the need to enforce a particular shape of the MODF.

The $\sin\ \gamma$ kernel in Eq. (8) can be expanded as a Legendre series and the explicit dependence on the molecular orientations determined using the addition theorem for Legendre polynomials. Substituting Eq. (17) into Eq. (6) and performing the necessary integrations gives

$$\sigma[f] + C\rho[f] = 2\pi \int \sum_{n=0}^{\infty} a_{2n}P_{2n}(\cos\ \theta_i)\ln[a_{2n}P_{2n}(\cos\ \theta_i)] \times d\cos\ \theta_i + C16\pi^2 \sum_{n=0}^{\infty} \frac{2}{4n+1}a_{2n}^2 C_{2n} \quad (18)$$

for the contribution to the free energy from the spherocylinders. The first term on the right hand side of this equation has no analytical form; however, the integral is evaluated numerically using a 64 point Gaussian quadrature.

In order to carry out these integrals it is necessary to assume that the director of the nematic phase is coincident with the z axis of an arbitrary Cartesian framework. The last term in Eq. (15) also depends on the molecular orientation, however, in its present form the external field is coincident with the z axis. Using the addition theorem for Legendre polynomials the field orientation and molecular orientation can be decoupled within the framework that the nematic director lies along the z axis. Equation (17) can be substituted into Eq. (15) and the necessary integrals performed, giving

$$\frac{A_1^{DD}}{kT} = \frac{2\mu B_0}{kT}L(\alpha) - \frac{\mu_0\mu^2}{r_d^3 kT 4\pi}L(\alpha)^2\frac{2}{5}a_2P_2(\cos\ \theta_B) \quad (19)$$

as the full dipolar contribution to the free energy. At this point the explicit orientational dependence of the nematic director and the field orientation becomes apparent.

The full Helmholtz free energy is given by

$$\frac{A}{NkT} = \frac{A^{ideal}}{NkT} + \sigma(f) + C16\pi^2\sum_{n=0}^{\infty}\frac{2}{4n+1}a_{2n}^2C_{2n} + \ln\left(\frac{\alpha}{\sinh\alpha}\right) + \alpha L(\alpha) + \frac{2\mu B_0}{kT}L(\alpha) - \frac{\mu_0\mu^2}{r_d^3kT4\pi}L(\alpha)^2\frac{2}{5}a_2P_2(\cos\ \theta_B) \quad (20)$$

and is a function of a set of unknown parameters α and a_{2n}. In order to obtain the thermodynamic properties the free energy must be minimized with respect to all these parameters. In this work the free energy is minimized directly using the simplex algorithm described in Numerical Recipes [19].

Having minimized the free energy, the thermodynamic properties, pressure P, chemical potential μ_{cp} and mean magnetic moment M_B of the nematic and isotropic phases can be determined using the usual thermodynamic relationships,

$$P = -\left(\frac{\partial A}{\partial V}\right)_{B_0,N,T},$$

$$\mu_{cp} = \left(\frac{\partial A}{\partial N}\right)_{B_0,V,T}, \quad (21)$$

$$M_B = \left(\frac{\partial A}{\partial B_0}\right)_{N,V,T}.$$

The order parameter P_2, which is defined as

$$P_2 = \int f(\Omega_1)P_2(\cos(\theta_1))d\Omega_1 = \frac{2}{9}a_2, \quad (22)$$

is used to describe the bulk orientational order in the nematic phase. The phase transition between phases can be determined by ensuring that the pressure, chemical potential, and temperature of the coexisting phases are equal.

For practical reasons the Legendre series in Eq. (20) must be truncated at some finite number. Lasher [16] and Lekkerkerker [17] have both examined the convergence of the thermodynamic properties at the isotropic-nematic phase transition with respect to the truncation of the Legendre series. They found that convergence was achieved at $n=7$, however, Lekkerkerker reports a slight discrepancy between the coexisting nematic density obtained in his work and the results obtained by Lasher. Using the simplex method to directly minimize the free energy we found the same discrepancy at $n=7$, however, at $n=8$ our results converge to the same values as those reported by Lekkerkerker.

Although fields of the order of 14 T are required to drive the isotropic-nematic phase transition [20] it is common to find that the director of a typical nematic liquid crystal will

be aligned parallel or perpendicular to a much weaker external field [1,21]. A number of studies have examined the effect of an external field on the isotropic-nematic phase transition in a fluid of hard rods using the Onsager theory [20,22–24] and the decoupling approximation of Parsons [25]. In these studies, based upon the assumption that the nematic will align with the field, the field is assumed to couple directly to the principle axis of the molecule through the following dependence:

$$U_{field}(\theta) = -A\cos^2\theta, \tag{23}$$

where θ is the angle between the field and the molecular orientation and A is a constant that depends upon the nature of the field, e.g., magnetic, electric or flow field. In the case of the magnetic field $A=\Delta\chi B_0^2/2$, and $\Delta\chi$ is the anisotropy of the diamagnetic susceptibility of a single particle. The $\cos^2$ form of Eq. (23) is similar to dipolar coupling term in Eq. (19), however, Eq. (19) depends upon the mean magnetic moment per molecule, the dipole-dipole separation, and the orientation of the vector joining the two dipoles, which, in this case, happens to be the same as the molecular orientation.

In these previous reports the field is always considered to be aligned with the nematic director. In contrast, the results obtained by Kreis and Boesch [3] and Asllani and coworkers [4,6,7] have demonstrated an angular dependence of the dipolar coupling, which suggests that *in vivo*, the director is constrained to a particular direction. This feature occurs as an implicit part of the current model and is introduced through the dipole-dipole interaction term.

In order to provide results in dimensionless units the diameter of a spherocylinder is used to scale all other distance measure, i.e., $R=r_d/D$. In addition an energy parameter ε is introduced, this provides a dimensionless density $C=(L/D)\eta$ where η is the packing fraction $N\nu_o/V$ and υ_o is the cylinder volume $\pi D^2L/4$, a dimensionless temperature, defined as $T^*=kT/\varepsilon$, dimensionless pressure $P^*=P\nu_o/kT$, dimensionless chemical potential $\mu^*_{\mathrm{CP}}=\mu_{\mathrm{CP}}/kT$ the squared dimensionless dipole moment, $\mu^{*2}=\mu^2\mu_0/(4\pi D^3\varepsilon)$, dimensionless mean magnetic moment $M^*=M_B\sqrt{\mu_o/(4\pi D^3\varepsilon)}$, and the dimensionless field strength $B^*=B_0\sqrt{4\pi D^3}/\sqrt{\mu_0\varepsilon}$. The dimensionless dipolar coupling is defined as $b^*=b\hbar/kT$, where $b=-\mu_0\mu^2/4\pi r_d^3$ is the dipolar coupling measured in Hz.

RESULTS

Results for field aligned with nematic director

To make a comparison with previous studies, we consider the case when the field and the nematic director are aligned. In this configuration the fluid of hard spherocylinders develops orientational order even at low densities. Figure 2(a) shows the change in the order parameter, as the density is increased from the isotropic limit through the phase transition to the strongly ordered nematic phase at a number of different field strengths. There is no order-disorder phase transition as there is when the field is zero, however, if the pressure-density isotherm is followed at constant field and dipole moment a van der Waals–like loop is observed for

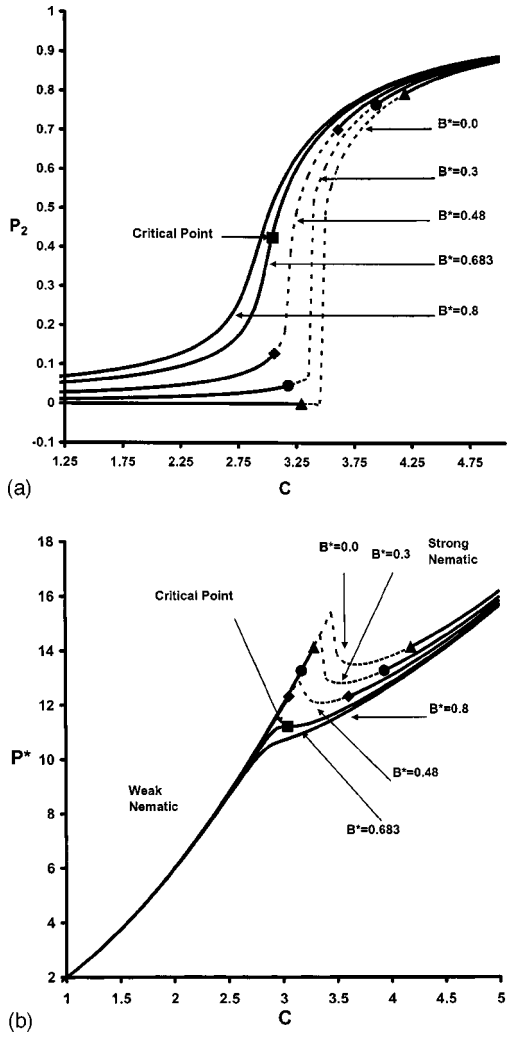

FIG. 2. Order parameter P_2 (a) and dimensionless pressure P^* (b) plotted as a function of the dimensionless density C for a range of field strengths B^*, with $\mu^*=1.0$ and temperature $T^*=1.0$. The field is aligned parallel to the nematic director.

field strengths up to a critical value, Fig. 2(b). Beyond the critical field a single nematic phase is observed in which the order parameter increases with the fluid density. This loop is characteristic of a first order phase transition. By solving the coexistence criteria, Eq. (21), the densities between the two coexisting phases can be determined at different field strengths. The isotropic-nematic phase transition appears to be replaced by a transition between a weakly ordered nematic phase and a strongly ordered nematic phase. To distinguish between these two phases we adopt the nomenclature of Varga *et al.* [24] and refer to the weakly ordered phase as the paranematic phase.

Fig. 3(a), shows the coexisting densities of the paranematic and nematic phases as a function of the field strength. In this calculation the temperature and dipole moment were fixed at 1. The figure shows a shift of the phase transition from higher to lower densities in both phases as the field is increased. It also shows a decrease in the density jump at the phase transition up to a critical point $B^*=0.683$, after which only the single nematic phase exists. Figure 3(b) shows the

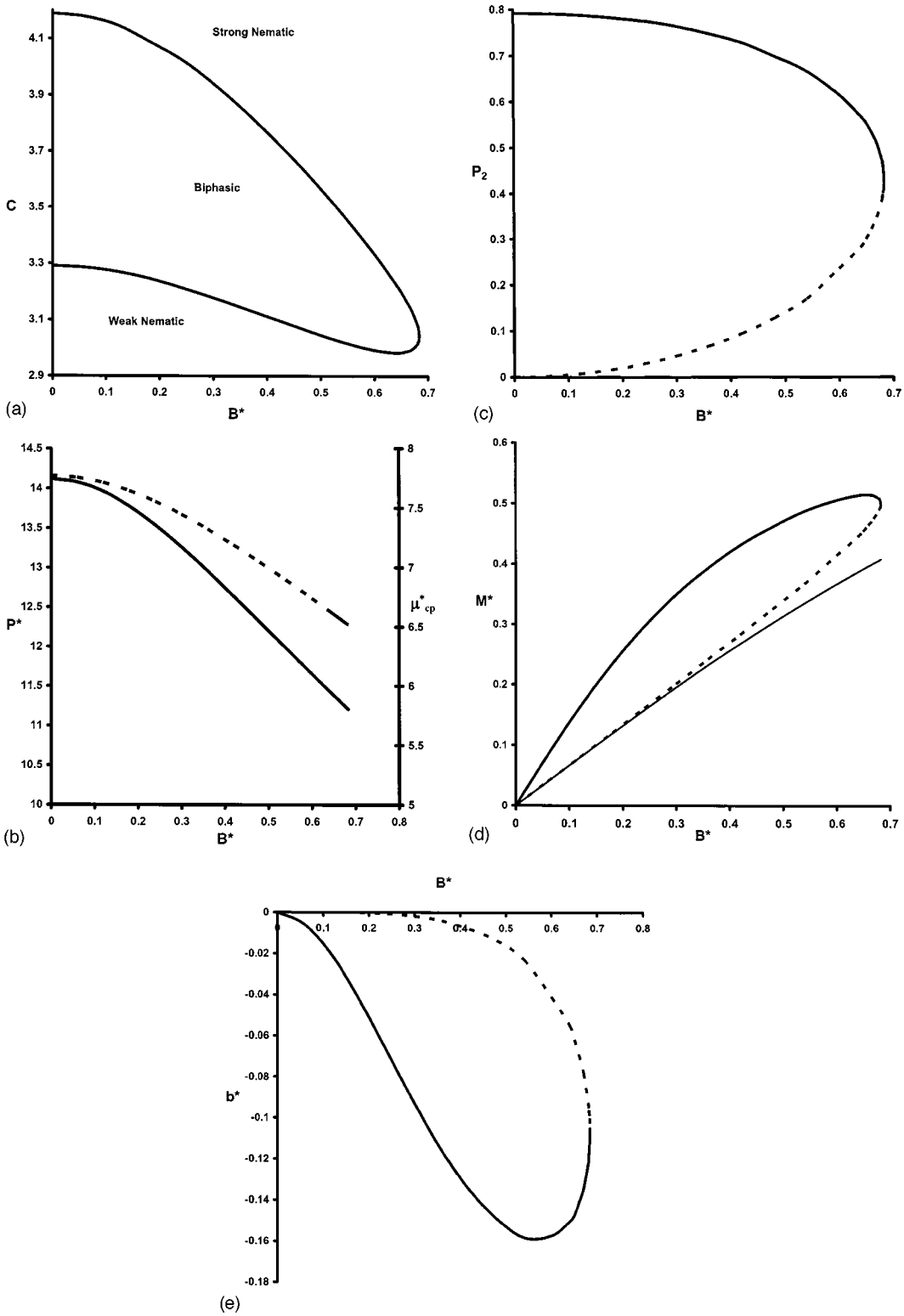

FIG. 3. Phase behavior with the field and nematic director aligned. (a) Dimensionless density C–field strength B^* projection of the phase diagram for spherocylinders with magnetic dipoles at constant dipole moment, with the same temperature and dipole moment as Fig. 2. The black line shows the coexisting densities of the weakly order paranematic phase and the strongly ordered nematic phase. (b) Dimensionless pressure P^* (solid line) and dimensionless chemical potential (dashed line) of the coexisting phases plotted as a function of field strength. (c) Order parameter P_2 in the paranematic phase (broken line) and nematic phase (solid line) at the phase transition plotted as a function of field strength B^*. (d) The dimensionless mean magnetic moment in the paranematic (broken line) and nematic (solid line) coexisting phases plotted as a function of field strength. The faint solid line represents the mean magnetic moment in an isotropic phase at the same density as the paranematic phase. (e) Dipolar coupling in the coexisting paranematic (broken line) and nematic (solid line) phases.

transition pressure and chemical potential as a function of field strength. Both the pressure and chemical potential move to lower values as the field strength is increased. In the case of the pressure, where there is no contribution from the dipoles, this effect can be accounted for due to the phase transition shift to lower densities. In the case of the chemical potential the decrease is partly due to the decrease in the transition density and partly due to the increased negative contribution from the dipoles. Both plots end at the critical point.

Figure 3(c) shows the orientational order parameter in the two coexisting phases at the phase transition. It is quite clear from this plot that the phase transition happens between a paranematic phase and a more strongly ordered nematic phase, at field strengths that are one third of the critical field or less. In fact, at these field strengths the paranematic phase is almost isotropic. As the field strength increases, the order in the paranematic phase increases quite rapidly while the coexisting nematic phase becomes less ordered. The two meet at the critical point where the order in both phases is identical.

It is gratifying to note that despite the alternative description of the coupling between the intramolecular dipoles and the external field the results obtained for the general phase diagram are identical to those reported in similar works [20,22–24]. This suggests that the current model does not provide any less information than previous studies with the additional advantage that we are able to explore the changes in the bulk magnetization and the dipolar coupling as a function of the molecular phase.

Figure 3(d) shows the mean magnetic moment per dipole in the two coexisting phases. It also shows the mean magnetic moment for the isotropic phase at the coexistence density of the paranematic phase. As may be predicted from the results in Fig. 3(c), at low field strengths where there is virtually no orientational order, the mean magnetic moment is almost equal to its isotropic value. As the field increases and the order increases, the mean magnetic moment is found to be larger than in the equivalent isotropic phase. This is relatively simple to understand. The dipoles are experiencing two effects, first a tendency to align with the field which results in the mean magnetic moment observed in the isotropic phase, second the dipoles have a tendency to align nose to tail, along the vector connecting the dipole centers. When the angle between the field and the director is zero, the two effects are acting in concert, resulting in an increase in the mean magnetic moment. In the nematic phase, the mean magnetic moment is much larger than the isotropic value. Again this is a direct consequence of the much stronger orientational order. The mean magnetic moment appears to increase almost linearly in the weakly ordered phase, however, in the strongly ordered phase there are two competing effects that account for the shape of the curve. In the first case as the field strength is increased, the mean magnetic moment will increase, as expected. As the phase transition moves to lower densities, the order in the nematic phase decreases, resulting in a decrease in the dipolar coupling contribution. Thus at low fields, the mean magnetic moment increases more rapidly than at field strengths closer to the critical field.

Figure 3(e) shows the dipolar coupling in the two coexisting phases. Both the orientational order and the mean magnetic moment contribute to the dipolar coupling, initially this results in a rapid increase in the magnitude of the coupling in both phases as the field strength is increased. At field strengths close to the critical field the order in the nematic phase decreases and the mean magnetic moment increases more slowly. This results in a decrease in the magnitude of the coupling in the nematic phase while the coupling continues to increase in the paranematic phase.

It is important to note that contribution to the Helmholtz free energy from the dipolar coupling and the dipole-field coupling are linked, such that the minimum in the free energy is a balance between these contributions and the free energy of the hard spherocylinder reference fluid.

Figure 4(a) shows the density dependence of the mean magnetic moment at constant field, dipole moment, and temperature. For noninteracting dipoles the mean magnetic moment would not be expected to depend upon density and this certainly is the case in the isotropic phase. However, as the fluid develops orientational order, with the field aligned with the director, the dipolar coupling term becomes nonzero, promoting the alignment of dipoles with the field. The density variation of the dipolar coupling is shown in Fig. 4(b). As expected from Eq. (24) the change in magnitude of the dipolar coupling shows a similar shape to the density dependence of the order parameter. This dependence is also mirrored in the mean magnetic moment. It is quite apparent from Figs. 2(a), 4(a), and 4(b) that the density dependence of the bulk magnetic properties arises purely from the density dependence of the order parameter. What is less clear is why the mean magnetic moment should have a linear dependence on order parameter, Fig. 4(c), despite the nonlinear minimization of the Helmholtz free energy with respect to the DODF. Since the mean magnetic moment has this linear dependence it might be expected that the dipolar coupling would also have a linear dependence, especially considering the relationship in Eq. (19). However, as show in Fig. 4(d) the relationship between the order parameter and dipolar coupling is rather more complicated, undoubtedly a consequence of the subtle interaction between the various contributions to the free energy minimization.

Results for field perpendicular to the nematic director

Figure 5(a) shows the dependence of the coexisting phases at the isotropic-nematic phase transition on field strength when the field is perpendicular to the nematic director. In contrast to the previous results, increasing the magnetic field shifts the phase transition to higher densities. The densities and the gap between the two coexisting phases both increase. The phase diagram does not exhibit critical behavior. This change in transition densities occurs because the second Legendre polynomial has the value -0.5 at 90° and the contribution to the Helmholtz free energy becomes positive. A decrease in the order parameter decreases the magnitude of the dipolar coupling which, in this case, reduces the free energy.

Figure 5(b) shows the order parameter in the nematic phase in the coexistence density at the phase transition. The most apparent difference between this figure and Fig. 3(c) is

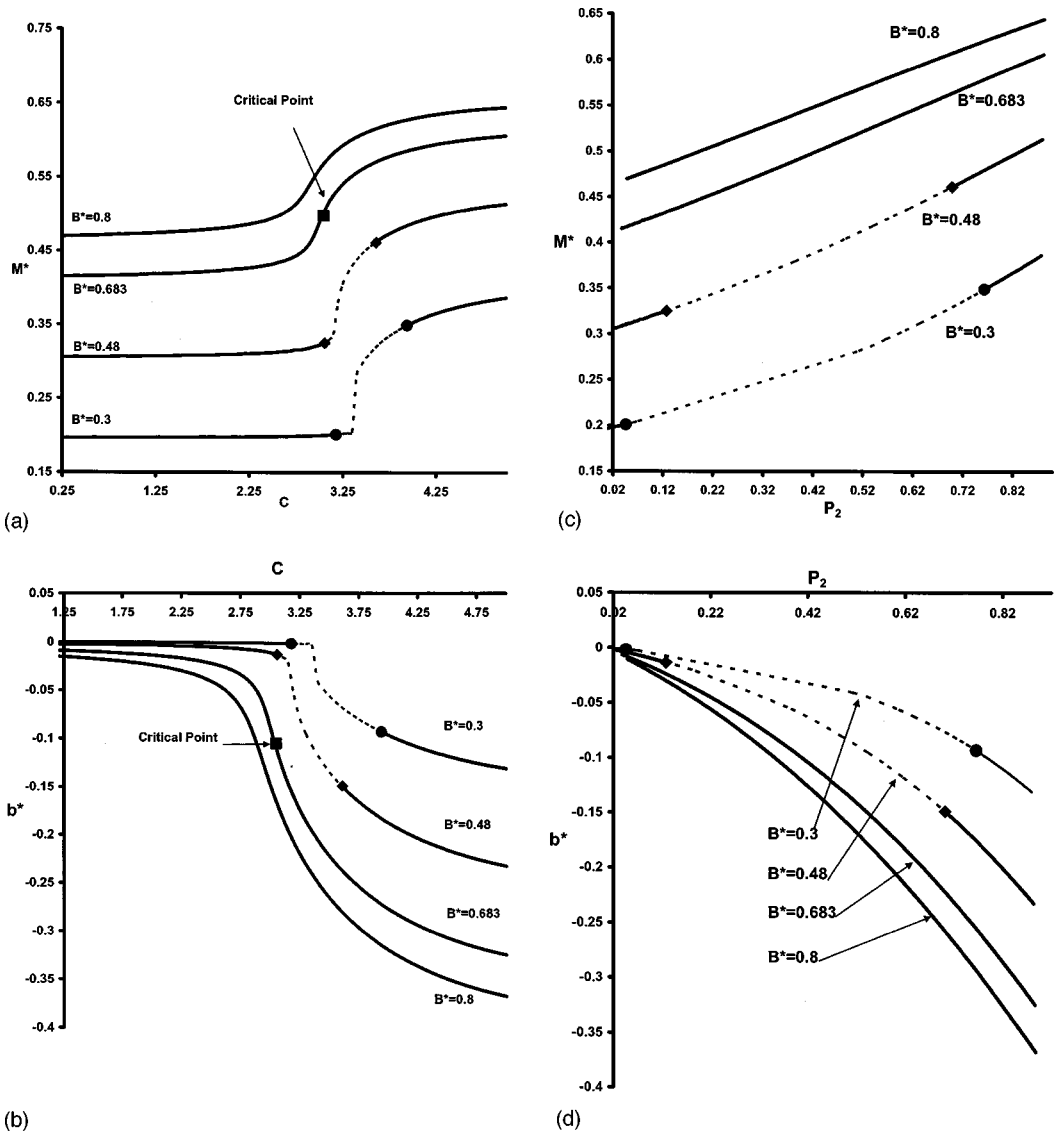

FIG. 4. The density dependence of the mean magnetic moment M^* (a) and the dipolar coupling (b) at variable field strength with the same temperature and dipole moment as Fig. 2. The dependence of the mean magnetic moment (c) and the dipolar coupling (d) on the orientational order parameter P_2 at the same temperature and dipole moment as (a) and (b) and variable field strength. The solid lines represent stable single phases and the broken lines metastable regions.

the absence of a paranematic branch. This is because the phase transition at all fields happens between a completely disordered isotropic phase and a nematic phase. There is no gradual increase in orientational order before the phase transition, as observed in the parallel case. As the transition density of the nematic phase increases with increasing field, the order parameter also increases. Although this theory does not take into account positionally ordered phases such as smectic liquid crystals or crystalline phase, it would be expected that the isotropic-nematic phase transition would be interrupted by a transition from the isotropic phase directly to a positionally ordered phase.

Figure 5(c) shows the field dependence of the transition pressure and chemical potential. As mentioned previously, the dipole interactions do not contribute to the pressure and predictably as the transition density rises, the transition pressure also rises. On the other hand, the dipole interactions do contribute to the chemical potential and as these negative contributions increase in magnitude with increasing field. The shift in transition density is relatively small in comparison to the previous results and the change in dipole contribution dominates the change in the chemical potential. This results in the observed decrease in the chemical potential.

Figure 5(d) shows the mean magnetic moment in the two coexisting phases. The isotropic phase has usual Langevin behavior with the parameter $\alpha = 2\mu B_0/kT$. The nematic phase shows a significant decrease in the mean magnetization at the phase transition. This occurs as the order parameter becomes nonzero, and the dipolar coupling becomes positive and nonzero, which increases the free energy. This increase in the dipolar coupling is partly offset by a decrease in the mean magnetic moment. Of course the decrease in the magnetic moment results in a free energy penalty in the dipole-field term. The increase in the dipolar coupling in the coexisting

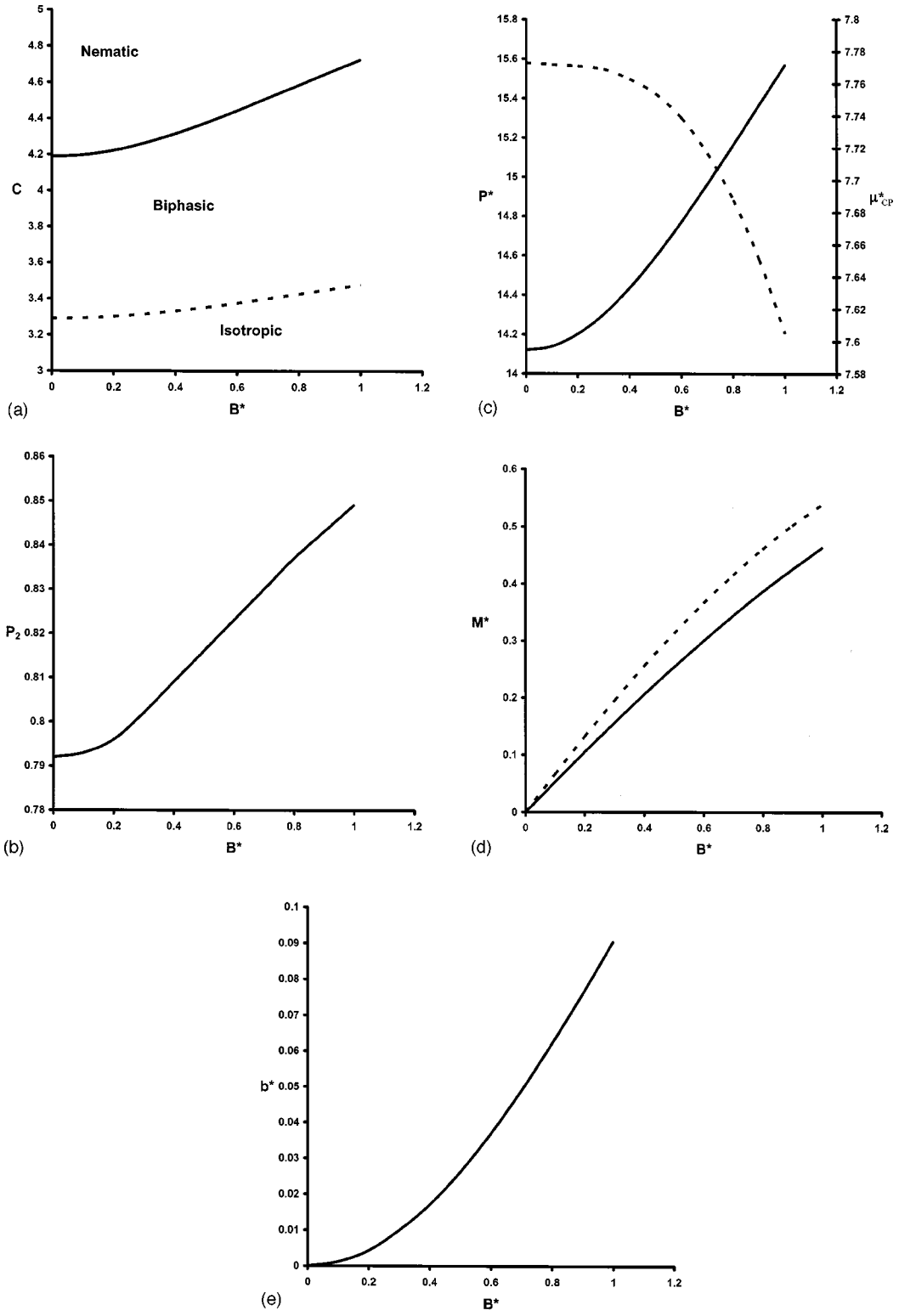

FIG. 5. Phase behavior with the field and nematic director perpendicular. (a) Dimensionless density C–field strength B^* projection of the phase diagram for spherocylinders with the same temperature and dipole moment as Fig. 2. The black line shows the coexisting densities of the isotropic phase and the nematic phase. (b) Order parameter P_2 nematic phase at the isotropic-nematic phase transition plotted as a function of field strength. (c) Dimensionless pressure (solid line) and dimensionless chemical potential (broken line) of the coexisting phases plotted as a function of field strength. (d) The dimensionless mean magnetic moment in the isotropic (broken line) and nematic (solid line) coexisting phases plotted as a function of field strength. (e) The field dependence of the dipolar coupling in the coexisting nematic phase.

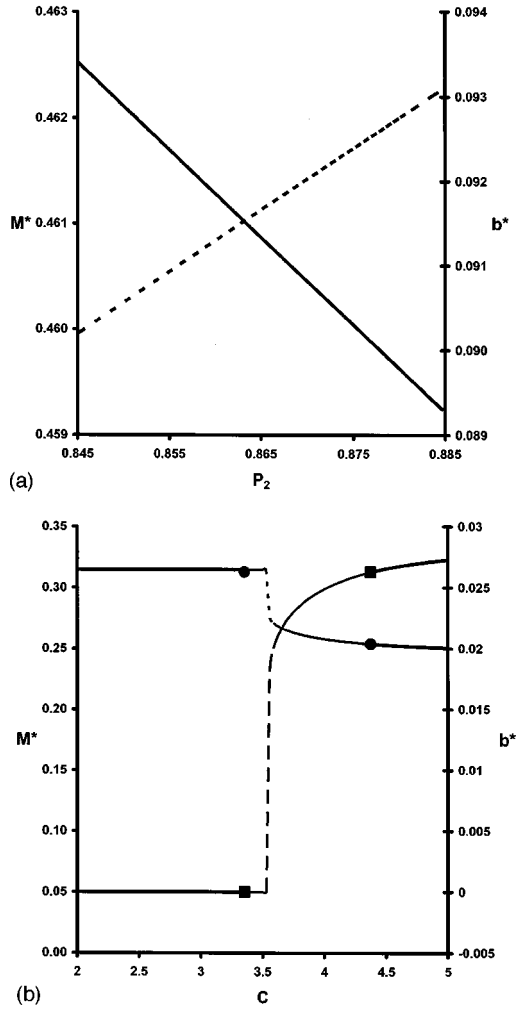

FIG. 6. (a) The dependence of the mean magnetic moment (solid line) and the dipolar coupling (broken line) on order parameter in the nematic phase with the field oriented perpendicular to the nematic director and constant dipole moment, $\mu^*=1.0$ and temperature $T^*=1.0$. (b) The density dependence of the mean magnetic moment (lines marked with a circle at the phase transition) and the dipolar coupling (lines marked with a square at the phase transition) with constant dipole moment, $\mu^*=1.0$ and temperature $T^*=1.0$ and the field oriented perpendicular to the nematic director.

nematic phase, occurring as the orientational order increases with field, is shown in Fig. 5(e).

As the field orientation changes from being parallel with the nematic director to being perpendicular, we have shown considerable differences in the thermodynamic and bulk magnetic properties of the spherocylinder fluid at the isotropic-nematic phase transition. These changes are also evident in the dependence of the bulk magnetic properties of the nematic phase on the order parameter, Fig. 6(a), and on the density, Fig. 6(b). In Fig. 6(a), we observe a linear decrease of the mean magnetic moment as a function of order, accompanied by a linear increase in the dipolar coupling. The magnitude of these changes is considerably smaller than those observed when the field and director are parallel, even at the higher field strength $B^*=1$, Fig. 6(a). The mechanism for these changes was discussed above. The dependence of the bulk magnetic properties on the density shown in Fig. 6(b) can also be easily understood from the previous discussion relating the density and the order parameter with the dipolar coupling and the mean magnetic moment.

Phase behavior at intermediate field orientations

The results for the parallel and perpendicular field alignments show two opposing phase diagrams, one in which the dipolar interactions stabilise the nematic phase with respect to the isotropic phase and the other in which the nematic phase is less stable. These two examples represent the extremes in the phase diagrams since the two orientations represent the maximum positive and negative values of the second Legendre polynomial. As the angle between the field and director is increased from the parallel alignment, we would expect that the absolute change in transition density would decrease, as the magnitude of the dipolar coupling term decreases and the critical point would shift to higher field. At the so-called magic angle, (54.74°) the dipolar coupling term will be zero and the isotropic-nematic transitions will be identical to the zero field case for all field strengths. Passing through the magic angle the dipolar coupling contribution to the free energy becomes positive, resulting in a destabilization of the nematic phase. This will produce phase behavior similar to that shown in Figs. 5 and 6, but with smaller changes in the parameters. At 90° the phase behavior will be as described previously.

Angular dependence of the dipolar coupling and mean magnetic moment

Figure 7(a) shows the angular dependence of the mean magnetic moment at various field strengths at a fixed density in the nematic phase. It is striking that there is a significant change in the mean magnetic moment from the parallel orientation to the perpendicular. At $B^*=0.2$ the ratio of the parallel to perpendicular moment is almost 3:1. Figure 7(b) shows the angular dependence of the mean magnetic moment at $B^*=0.2$ as the dipole moment is varied between 0.3 and 0.9. It becomes quite clear that the shape of the angular dependence curve is dominated by the strength of the dipole moment. This is to be expected since the dipolar coupling term, which contains the angular dependence, depends upon the dipole moment squared. Since the amplitude of the NMR signal is directly proportional to the mean magnetic moment, it may be possible to measure these changes of magnitude; however, for *in vivo* measurements of the signal originating from relatively small molecules this would be unlikely due to the small intrinsic dipole moment of a proton. On the other hand ferrocolloids [26], stable colloidal dispersions that have stable permanent magnetic dipoles, can have dipole moments that are orders of magnitude larger than the intrinsic moment of a proton. The angular dependence of the mean magnetic moment may be observable in these systems.

Figure 8 shows the angular dependence of the dipolar coupling, under the same conditions as in Fig. 7(a). Clearly all the curves exhibit a second Legendre polynomial–like

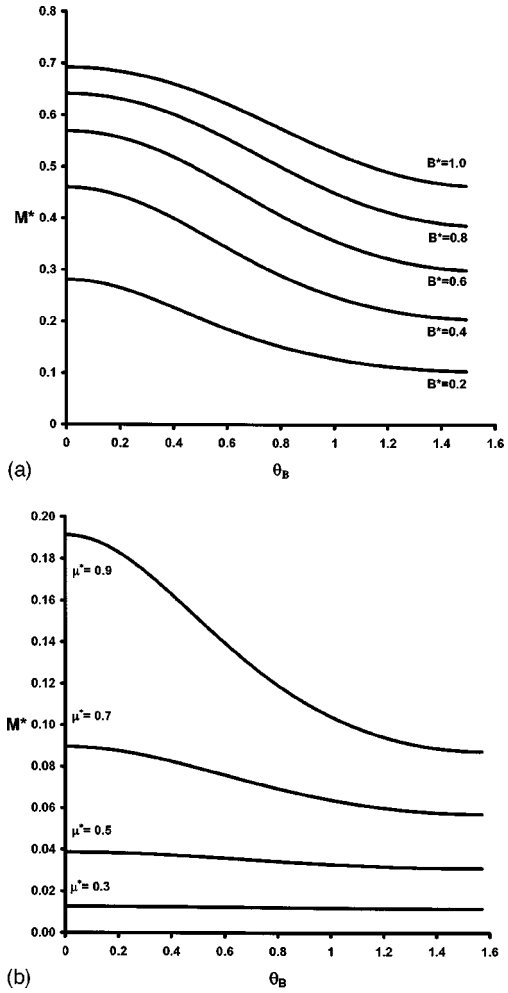

FIG. 7. Dependence of the mean magnetic moment on the angle between the field and the director at (a) variable field and fixed dipole moment $\mu^*=1.0$ and temperature $T^*=1.0$ and (b) at variable dipole moment and fixed field strength $B^*=0.2$ and temperature $T^*=1.0$.

shape, passing through zero at the magic angle. However, if this was the only influence on the shape of the curves, the ratio of the magnitude of the dipolar coupling at parallel alignment should be exactly twice the magnitude when the field and director are perpendicular. The two should also have opposite signs. This is not the case with the ratio of the two values ranging from almost 5:1 when $B^*=1.0$ to 15:1 when $B^*=0.2$. The reason for this variation in shape arises because the dipolar coupling is proportional to the square of the mean magnetic moment. As well as changing the shape of the curve, this suggests that the dipolar coupling should exhibit a significant dependence on field strength. Such a suggestion is rather contentious since the dipolar coupling is often reported as being independent of field strength. Initially, this would appear to be the case since Eq. (3), does not contain an explicit dependence on field strength. However, the statistical mechanical ensemble average of this property has been shown to depend on the mean magnetic moment, as described previously, and this explicitly depends upon the field strength.

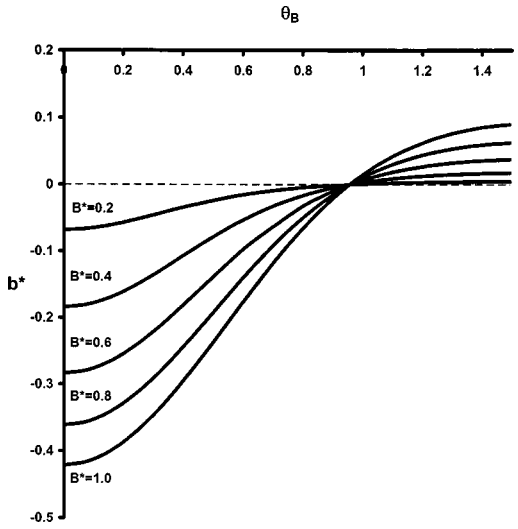

FIG. 8. Dependence of the dipolar coupling on the angle between the field and the director θ_B at variable field strength and fixed dipole moment $\mu^*=1.0$ and temperature $T^*=1.0$.

Modeling the dipolar coupling from *in vivo* MR spectroscopy

Almost a decade ago, Kreis and Boesch reported measurements of the dipolar coupling obtained from the calf muscle of a human volunteer [3]. The nonzero dipolar coupling suggested that there was some level of molecular ordering. However, the measurements did not show the broad powderlike spectra that would be expected from a crystalline structure. The authors concluded that almost complete motional averaging was taking place but that there was incomplete orientational averaging. These observations suggest that the signal obtained originated from a nematic liquid crystal. Measurements were taken with the subject's leg positioned at ten different orientations to the main magnetic field. The dipolar coupling observed for a particular pair of peaks was found to change as the orientation of the leg changed. This suggested that there was a constraint on the preferred direction of orientation, since bulk liquid crystalline phases will tend to align, even with relatively weak magnetic fields

In order to support the conclusion of Kreis and Boesch that the features of the NMR spectra they obtained may be attributed to a nematic liquid crystal, it is useful to fit the dipolar coupling data to results obtain from this theoretical approach. To do this it is necessary to convert the dimensionless dipolar couplings to values in Hz. This is achieved by multiplying by $kT/\hbar$ ($\hbar$=Planck's constant divided by 2π). To perform the fitting on such a relatively small data set it is also necessary to reduce the number of parameters. From Eq. (19) it is clear that the temperature is a scaling factor that has the same effect on both the dipole-field term and the dipole coupling term. It is therefore convenient to define a dimensionless temperature $T^*=1$ giving $\varepsilon=kT$. It is also known that the data were collected at 1.5 T, assuming a dipole separation of 0.2 nm and a dimensionless separation, $R=1$, it is possible to obtain the reduced field strength of $B^*=0.0186$. The dipole separation is allowed to vary but the separation in nanometres is assumed to be constant, so changes in the

TABLE I. Parameters obtained from fitting the dipolar coupling obtained from the theory to the experimental data of Kreis and Boesch [3]. C is the dimensionless density, ϕ is the angle between the orientation of the muscle fibers and the tibia or fibula, μ^* is the dimensionless dipole moment, R^* is the dimensionless separation between the dipoles in a single molecule, B^* is the dimensionless field strength, and P_2 is the order parameter in the model fluid. The fitting was carried out at a dimensionless temperature $T^*=1$.

C	ϕ (rad) [deg]	μ^*	R^*	B^*	P_2
4.204	−0.0916 [−5.248]	0.0075	1.006	0.183	0.793

dimensionless separation result in a change of the scaling parameter D. In order to keep a fixed field, the dimensionless field strength must be rescaled as D changes.

As pointed out by Kreis and Boesch, the angle measured in their experiment was obtained from MR images and were the angles between the magnetic field and the tibia or fibula. This is not necessarily the orientation of the nematic director. To account for a simple shift between the measured angle and the director orientation a parameter ϕ is introduced. The fitting was performed at human body temperature, approximately 311 K, with the dimensionless dipole moment and the density used as fitting parameters. The parameters were obtained from the fitting are shown in Table I and the results of the fitting shown in Fig. 9. The results of the fitting show excellent agreement between the experimental and theoretical results. Importantly the density obtained is greater than the transition density and therefore lies in a region of the phase diagram where the nematic phase is the thermodynamically stable phase. This lends some theoretical support to the conclusions drawn by Kreis and Boesch. In addition, the order parameter obtained from the fitting is considerably larger than their value, reinforcing the suggestion that the origin of the NMR signal is an orientationally ordered phase. An estimate of the intrinsic dipole moment may be obtained from the fitting results. This was found to be 4.397×10^{-24} J/T, a value that is rather large. However, such a result should be expected considering the simplicity of the model and the absence of a realistic molecular structure. The shift angle ϕ is found to be very close to the value obtained by Kreis and Boesch.

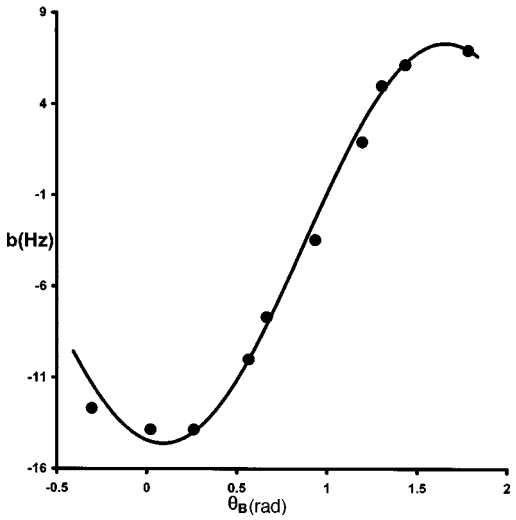

FIG. 9. Theoretical dipolar coupling b plotted as a function of the angle between the field and the director obtained by fitting the theory (solid line) to the dipolar coupling data obtained by Kreis and Boesch [3] (filled circles).

Despite the simplicity of the model, the results suggest that the current model could be used to map changes in the dipolar coupling due to pathological changes in the muscle tissue to density changes in the model fluid. However, in using this model to describe the dipolar coupling observed in the spectra of human muscle one must imagine that the interaction of the molecules with the physical environment is giving rise to a potential of mean force which is adequately described by a single component model fluid. The results presented in this work suggest that this model is sufficient to describe the dipolar coupling, however, it does not provide a great insight into the changes in muscle structure that might give rise to the observed changes in the MR signal, beyond establishing the fact that the freely moving molecules experience partial orientational averaging.

It is more likely that this simple model will be of use as a model of the probe molecules in a theory where the muscle fiber environment is more explicitly described. The fitting process could subsequently be used to relate changes in the spectroscopic data to changes in fiber density and orientation.

CONCLUSIONS

In this work the effects of an external magnetic field on the isotropic-nematic phase transition of the fluid of hard spherocylinders with a pair of freely rotating embedded magnetic dipoles are examined. The work takes into account the coupling between the external field and the dipoles, and the coupling between dipoles in the same molecules. This is in contrast to a number of other studies where the coupling between the molecular magnetism and the external field is effectively modeled through anisotropy in bulk magnetic susceptibility, aligned along the major molecular axis. The model presented here provides a way to understand the dependence of the bulk dipolar coupling, a property that can be measured using NMR spectroscopy and the orientational order in the liquid crystalline fluid.

When the external magnetic field and the nematic director are aligned the fluid exhibits phase behavior that is very similar to the phase behavior observed in previous studies with the isotropic-nematic phase transition being replaced with a transition between a weakly ordered nematic phase and a more strongly ordered phase. As the field is increased the first order phase transition gives way to a single continuous nematic phase at a critical field strength. It is clear from these results that the new model can still account for the phase behavior described in previous studies, however, parallel alignment can be considered a single example of this more general model.

In contrast to the parallel case, when the field and director are perpendicular the nematic phase is destabilized with re-

spect to the isotropic phase and the phase transition moves to higher densities as the field strength is increased. In this case, at all field strengths the transition is between the orientationally ordered nematic phase and the disordered isotropic phase. At intermediate orientations the effect of the field is weaker and in fact has no effect at the magic angle, 54.74°, when the dipolar coupling contribution to the free energy becomes zero, regardless of the strength of the orientational order in the fluid. When the field-director orientation is greater than the magic angle, the phase behavior is similar to that of the perpendicular case. When the orientation is less than the magic angle, the dipolar coupling term helps to stabilize the orientational order in the fluid and a phase diagram similar to the parallel case is observed.

In dimensionless units, the experimental conditions for ^{1}H NMR are likely to fall close to the zero field region of the phase diagram. In this region the orientational structure of the fluid exerts little influence on the mean magnetic moment and it is unlikely that the sensitivity of such an experiment could be significantly increased through the use of liquid crystal solvents. On the other hand, a great deal of work has been invested in the development of ferrocolloids [26] in which the dipole moment of the colloidal particle can be tailored. Such systems exhibit permanent dipole moments that are orders of magnitude larger than the intrinsic dipole moment of a proton. An understanding of the phase behavior of these systems is important in the development of engineering applications. From this point of view the magnetic spherocylinder fluid offers a useful reference model for such studies of phase behavior.

While the mean magnetic moment of an ensemble of protons may be insensitive to the changes in the orientation structure of a fluid, the dipolar coupling is not. Although this model is very simple, containing the minimum set of features to exhibit nematic phase behavior and to describe the effects of molecular structure on the bulk magnetic properties, it has still provided a useful model for fitting the experimental data obtained by Kreis and Boesch [3]. The results of the fitting returned a density in the region of the phase diagram where the nematic phase is stable and not the rather broad biphasic region where the nematic phase is metastable. As such, even in its current simplistic state the model provides a method for mapping the spectroscopy data to a model fluid. Despite the fact that spherocylinder fluid does not explicitly model the biochemical environment or the type of physical structure that might be envisioned in muscle, once it has been established that there is imperfect orientational averaging of the MR signal, the model is expected to describe the angular dependence of the dipolar coupling in a systematic manner. The systematic behavior may turn out to be useful in distinguishing between different pathologies. The model is particularly crude, since the orientation of the field is controlled by fixing a parameter in the free energy that would not be directly available to the experimenter in the same way that the bulk thermodynamic properties are, e.g., temperature, pressure, and volume. The original spectroscopic signal is thought to come from a relatively free moving molecule constrained by the highly ordered structure of the muscle fibers. The first step towards modeling this behavior was the development of this model for the freely moving molecules. The second stage and the subject of ongoing work is the development of a constraining environment, which could be used to describe changes in the MR signal as a function of the model muscle fiber density and orientation.

ACKNOWLEDGMENTS

We would like to acknowledge Dr. Paul Bromily and Professor Gareth Morris for their helpful discussion. D.C.W. would like to thank the Medical Research Council for financial support.

APPENDIX A: DERIVATION OF THE HELMHOLTZ FREE ENERGY

In order to derive an expression for the Helmholtz free energy we exploit the idea, originally proposed by Onsager, of treating molecules of a particular orientation as a distinct species [10]. This effectively decouples the integration of the partition function over the positions of the molecules from the integration over molecular orientations. This concept is extended to the orientation of the dipoles. From this a single species is defined by a particular molecular orientation Ω_{i} and two dipole orientations Ω_1, and Ω_2. The partition function $Q_{\mathrm{N}},(V,T,\Omega_{\mathrm{i}},\Omega_{\mathrm{j}}\Omega_1,\Omega_2)$ is factorized into three terms,

$$Q_N(V,T,\hat{\Omega}_i,\hat{\Omega}_j,\hat{\Omega}_1,\hat{\Omega}_2) = Q_N^{Ideal}[Q_1^{DD}(\hat{\Omega}_i,\hat{\Omega}_1,\hat{\Omega}_2)]^N \times Q_N^{Excess}(V,T,\hat{\Omega}_i,\hat{\Omega}_j). \quad \text{(A1)}$$

Q_N^{Ideal} is the well known ideal gas contribution that arises from the integration over the coordinates of momentum [15]. Since dipoles in different molecules are noninteracting, the dipole contributions do not depend upon the positions of the centers of mass of the molecules. As a result this contribution to the partition function can be obtained as the product of N dipole pair partition function $Q_1^{DD}(\hat{\Omega}_i,\hat{\Omega}_1,\hat{\Omega}_2)$. The final term $Q_N^{Excess}(V,T,\hat{\Omega}_i,\hat{\Omega}_j)$ is the contribution due to the hard spherocylinders themselves. In this work we derive this contribution following Onsager. The Helmholtz free energy A is obtained from the partition function through the standard expression for a Canonical ensemble,

$$A(\hat{\Omega}_i,\hat{\Omega}_j,\hat{\Omega}_1,\hat{\Omega}_2) = -kT \ln Q_N(V,T,\hat{\Omega}_i,\hat{\Omega}_1,\hat{\Omega}_2). \quad \text{(A2)}$$

Here k is the Boltzmann's constant. This leads to a decoupling of the free energy contributions,

$$\frac{A(\hat{\Omega}_i,\hat{\Omega}_j,\hat{\Omega}_1,\hat{\Omega}_2)}{NkT} = \frac{A^{ideal}}{NkT} + \frac{A_1^{DD}(\hat{\Omega}_i,\hat{\Omega}_1,\hat{\Omega}_2)}{kT} + \frac{A^{excess}(\hat{\Omega}_i,\hat{\Omega}_j)}{NkT}. \quad \text{(A3)}$$

The free energy of the full ensemble can now be written as the free energy of a mixture,

$$\frac{A}{NkT} = \sum x_i \ln x_i + \sum x_1 \ln x_1 + \sum_i \sum_j \sum_1 \sum_2 x_i x_j x_1 x_2 \frac{A(\hat{\Omega}_i, \hat{\Omega}_j, \hat{\Omega}_1, \hat{\Omega}_2)}{NkT}. \quad \text{(A4)}$$

In this x_i is the mole fraction of molecules with orientation Ω_i and x_1 is the mole fraction of dipoles with orientation Ω_1. The components of the mixture are not discrete, however, since the orientations of both the dipoles and the spherocylinders vary smoothly over all possible orientations. The result is that the summations in Eq. (A4) must be written as integrations over all possible molecular and dipolar orientations and the mole fractions continuous orientational distributions functions,

$$\frac{A}{NkT} = \int f(\hat{\Omega}_i) \ln f(\hat{\Omega}_i) d\hat{\Omega}_i + \int \rho(\hat{\Omega}_1) \ln \rho(\hat{\Omega}_1) d\hat{\Omega}_1 + \int\int\int\int \frac{A(\hat{\Omega}_i, \hat{\Omega}_j, \hat{\Omega}_1, \hat{\Omega}_2)}{NkT} \times \rho(\hat{\Omega}_1)\rho(\hat{\Omega}_2) f(\hat{\Omega}_i) f(\hat{\Omega}_j) d\hat{\Omega}_1 d\hat{\Omega}_2 d\hat{\Omega}_i d\hat{\Omega}_j, \quad \text{(A5)}$$

where the molecular orientational distribution is denoted as $f(\Omega_i)$ and the dipole orientational distribution function as $\rho(\Omega_1)$. In the case of linear dipoles and molecules, $d\Omega$ may be written as $d\cos\theta\, d\phi$ where θ is the polar angle and ϕ the azimuthal angle. The orientational distribution functions are normalized under the conditions $\int f(\hat{\Omega}_i) d\hat{\Omega}_i = 1$ and $\int \rho(\hat{\Omega}_i) d\hat{\Omega}_i = 1$.

Substituting Eq. (A3) into Eq. (A5) gives the overall expression for the Helmholtz free energy,

$$\frac{A}{NkT} = \int f(\hat{\Omega}_i) \ln f(\hat{\Omega}_i) d\hat{\Omega}_i + \int \rho(\hat{\Omega}_1) \ln \rho(\hat{\Omega}_1) d\hat{\Omega}_1 + \frac{A^{ideal}}{NkT^+} + \int\int \frac{A_1^{DD}(\hat{\Omega}_i, \hat{\Omega}_1, \hat{\Omega}_2)}{kT} \rho(\hat{\Omega}_1)\rho(\hat{\Omega}_2) f(\hat{\Omega}_i) d\hat{\Omega}_1 d\hat{\Omega}_2 d\hat{\Omega}_i + \int\int \frac{A^{excess}(\hat{\Omega}_i, \hat{\Omega}_j)}{NkT} f(\hat{\Omega}_i) f(\hat{\Omega}_j) d\hat{\Omega}_i d\hat{\Omega}_j. \quad \text{(A6)}$$

APPENDIX B: DERIVATION OF THE LANGEVIN FREE ENERGY FOR A GAS OF FREE MAGNETIC DIPOLES USING THE ONSAGER APPROACH

As described in Appendix A Onsager suggested that particles of different orientations could be considered as different species and the free energy for a freely rotating system could be derived as a mixture of different species. For a gas of freely rotating noninteracting dipoles with dipole moment μ moving in an external magnetic field **B** the Helmholtz free energy can be written as

$$\frac{A}{NkT} = \int \rho(\hat{\Omega}) \ln[\rho(\hat{\Omega})] d\hat{\Omega} - \frac{\mu B}{kT} \int \cos(\theta) \rho(\hat{\Omega}) d\hat{\Omega}, \quad \text{(B1)}$$

where all the symbols have the same means as described previously. For the dipoles the DODF does not depend on the azimuthal angle and under the assumption that the solid angle element is defined as $d\Omega = d\cos(\theta) d\phi / 4\pi$ it is possible to integrate out the azimuthal dependence in Eq. (B1) giving

$$\frac{A}{NkT} = \frac{1}{2} \int_{-1}^{1} \rho(\theta) \ln[\rho(\theta)] d\cos(\theta) - \frac{\mu B}{kT} \frac{1}{2} \int_{-1}^{1} \cos(\theta) \rho(\theta) d\cos(\theta). \quad \text{(B2)}$$

Substituting Eq. (13) as the functional form of the DODF and performing the required integrals we obtain

$$\frac{A}{NkT} = \ln\left(\frac{\alpha}{\sinh \alpha}\right) + \left(1 - \frac{\mu B}{kT} \frac{1}{\alpha}\right)(\coth \alpha - 1). \quad \text{(B3)}$$

It is reasonably straightforward to show that the minimum of this free energy expression with respect to the variable α occurs when $\alpha = \mu B / kT$. Substituting this result into Eq. (B3) gives

$$\frac{A^{\min}}{NkT} = \ln\left(\frac{\alpha}{\sinh \alpha}\right) \quad \text{(B4)}$$

which is exactly the Langevin free energy for a gas of noninteracting dipoles. The derivation of this free energy can be found in Refs. [13,15].

[1] J. W. Emsley and J. C. Lindon, *NMR Spectroscopy Using Liquid Crystal Solvents* (Permagon, Oxford, 1975).
[2] C. Boesch, NMR Biomed. **14**, 112 (2001).
[3] R. Kreis and C. Boesch, J. Magn. Reson., Ser. B **104**, 189 (1994).
[4] I. Asllani, E. Shankland, T. Pratum, and M. Kushmerick, J. Magn. Reson. **139**, 213 (1999).
[5] C. Boesch and R. Kreis, NMR Biomed. **14**, 140 (2001).
[6] I. Asllani, E. Shankland, T. Pratum, and M. Kushmerick, J. Magn. Reson. **152**, 195 (2001).
[7] I. Asllani, E. Shankland, T. Pratum, and M. Kushmerick, J. Magn. Reson. **163**, 124 (2003).
[8] D. Sandström, A. V. Komolkin, and A. Maliniak, J. Chem. Phys. **104**, 9620 (1996).
[9] B. Stevensson, A. V. Komolkin, D. Sandström, and A. Maliniak, J. Chem. Phys. **114**, 2332 (2001).
[10] L. Onsager, Ann. N.Y. Acad. Sci. **51**, 627 (1949).
[11] S. C. McGrother, D. C. Williamson, and G. J. Jackson, J. Chem. Phys. **104**, 6755 (1996).
[12] P. Bolhuis and D. Frenkel, J. Chem. Phys. **106**, 666 (1997).
[13] P. Langevin, J. Phys. **4**, 678 (1905).
[14] T. Kristóf and I. Szalai, Phys. Rev. E **68**, 041109 (2003).

[15] R. K. Pathria, *Statistical Mechanics* (Permagon, Oxford, reprint, 1988).
[16] G. Lasher, J. Chem. Phys. **54**, 4141 (1970).
[17] H. N. W. Lekkerkerker, P. Coulon, R. Van Der Haegan, and R. Deblieck, J. Chem. Phys. **80**, 3427 (1984).
[18] G. J. Vroege and H. N. W. Lekkerkerker, Rep. Prog. Phys. **55**, 1241 (1992).
[19] W. H. Press, S. A. Teukolsky, W. T. Vetterling, and B. P. Flannery, *Numerical Recipes in C*, 2nd ed. (Cambridge University Press, Cambridge, England, 1992).
[20] J. Tang and S. Fraden, Phys. Rev. Lett. **71**, 3509 (1993).
[21] G. R. Luckhurst and G. W. Gray, *The Molecular Physics of Liquid Crystals* (Academic Press, London, 1979).
[22] S.-D. Lee, J. Chem. Phys. **86**, 6567 (1987).
[23] A. R. Khokhlov and A. N. Semenov, Macromolecules **15**, 1272 (1983).
[24] S. Varga, G. Jackson, and I. Szalai, Mol. Phys. **93**, 377 (1998).
[25] J. D. Parsons, Phys. Rev. A **19**, 1225 (1979).
[26] R. E. Rosenweig, *Ferrohydrodynamics* (Cambridge University Press, Cambridge, England, 1985).